The Warm Season Dip in Diurnal Temperature Range over the Eastern United States

IMKE DURRE AND JOHN M. WALLACE

Department of Atmospheric Sciences, University of Washington, Seattle, Washington

(Manuscript received 1 November 1999, in final form 1 April 2000)

ABSTRACT

In light of numerous studies documenting a decline in the diurnal temperature range (DTR) over much of the globe, some authors have in recent years examined the annual march of the DTR in an effort to understand better the factors that influence the DTR's seasonal variations. These papers show that, over the southern two-thirds of the eastern United States, the DTR's climatology features peaks in spring and autumn and minima in winter and mid-to-late summer. However, the factors responsible for these characteristics remain uncertain. In this study, the DTR climatology of the eastern United States is analyzed in detail using daily surface and 850-mb data, with emphasis on possible relationships to seasonal changes in vegetation. It is shown that the warm season dip in the DTR deepens and widens from north to south across the study area, in accordance with a lengthening of the growing season. Furthermore, the dip is particularly prominent in the annual march of the DTR on mostly sunny days, indicating that seasonal variations in cloudiness are not responsible for this feature. The climatologies of daily maximum and daily minimum temperatures are found to be very different from each other: the former flattens out after the springtime peak in the DTR whereas the latter exhibits a pronounced mid-to-late summer maximum. These findings suggest that, by inhibiting daytime surface heating, evapotranspiration from vegetation contributes significantly to the dip in the DTR during the warm season in the eastern United States.

1. Introduction

In recent years, Robinson et al. (1995) and Leathers et al. (1998) have demonstrated that the shape of the annual cycle of the diurnal temperature range (DTR) varies across the contiguous United States. Over much of the west as well as the northern tier states (regions 1 and 3 in Leathers et al.), the DTR peaks during summer and reaches its minimum during the winter. From the central and southern Great Plains eastward to the Atlantic Ocean (region 2 in Leathers et al.), however, the DTR climatology exhibits two comparable maxima, one during spring and one during autumn, that are separated by a distinct, broad summer minimum. The characteristic double peak is not well-simulated by general circulation models: between spring and autumn, the seasonal variations in the DTR tend to be smaller in the models than in the observations (Kukla et al. 1995; Mearns et al. 1995). In light of the widespread decrease in the DTR over the past several decades and its possible relationship to human activities (e.g., Karl et al. 1993), the correct simulation of the DTR by climate models is of major importance.

An understanding of the reasons for the discrepancy between models and observations may be gained by examining the factors that influence seasonal changes in the DTR over the eastern United States. In general, the DTR is affected by diurnally asymmetric forcings, that is, forcings whose magnitude or sign varies with the time of day. Observational and modeling studies have shown that shortwave radiative forcings tend to exhibit a greater diurnal asymmetry than longwave forcings, primarily because the diurnal cycle of solar radiation is considerably more pronounced than the diurnal cycle of thermal radiation (Stenchikov and Robock 1995; Campbell and Vonder Haar 1997; Dai et al. 1999). Solar forcings that may affect seasonal changes in the DTR by modulating daily maximum temperature include insolation, the reflection of solar radiation by clouds, and the surface albedo (Ruschy et al. 1991; Karl et al. 1993). Numerical experiments with radiative-convective models have suggested that the absorption of solar radiation by water vapor may also be a factor (Cao et al. 1992; Stenchikov and Robock 1995), but comprehensive analyses of surface and satellite-based observations by Campbell and Vonder Haar (1997) and Dai et al. (1999) provide little evidence of such an effect.

Surface evapotranspiration, which depends largely on net incoming solar radiation and the amount of moisture available for evaporation, can inhibit the rise in temperature during the day through evaporative cooling of the surface, but has little, if any, effect on nighttime temperatures (Cao et al. 1992; Verdecchia et al. 1994; Mearns et al. 1995; Dai et al. 1999). Observational ev-

Corresponding author address: Imke Durre, National Climatic Data Center, 151 Patton Ave., Ashville, NC 28801.
E-mail: idurre@ncdc.noaa.gov

idence for a lower DTR in the presence of higher evapotranspiration rates has been presented by Dai et al. (1999). Furthermore, both empirical and theoretical studies have demonstrated that evapotranspiration rates of the soil are higher and the DTR is lower over vegetated surfaces than over bare soil (Saltzman and Pollack 1977; Oliver et al. 1987; Radersma and de Reider 1996; Xue et al. 1996). Seasonal variations in evapotranspiration rates may occur in response to changes in solar radiation, precipitation, and the growth and senescence of vegetation (Kaufmann 1984; Dorman and Sellers 1989).

By trapping outgoing longwave radiation, atmospheric water vapor and clouds contribute significantly to the longwave radiative forcing of daily mean surface air temperature. However, diurnal variations in these forcings appear to be small at best. Based on monthly means of satellite-measured radiative fluxes and surface observations of daily maximum and minimum temperature, Campbell and Vonder Haar (1997) showed that the longwave radiative forcing of clouds produces an approximately equal warming in daytime and nighttime temperatures. In an extensive analysis of global daily station observations, Dai et al. (1999) found that when only clear days are considered, the DTR is largely unaffected by variations in the longwave radiative flux and specific humidity at the surface since both maximum and minimum temperatures tend to be warmer under more humid conditions. The results of these observational studies are supported by numerical experiments conducted by Mearns et al. (1995) and Stenchikov and Robock (1995). Unless seasonal changes in humidity and cloudiness are themselves diurnally asymmetric, their longwave radiative forcings will have little affect on the annual march of the DTR. Both Gaffen and Ross (1999) and Dai et al. (1999) have found the diurnal cycle of surface specific humidity to be small during all seasons. Thus, seasonal variations in the longwave radiative effects of atmospheric water vapor are unlikely to exert a significant influence on the DTR.

The rise in the climatological-mean diurnal temperature range from winter up to the time of the spring maximum has been attributed to a decrease in surface albedo as a result of the disappearance of snow cover (Ruschy et al. 1991; Schwartz 1996), an increase in net incoming solar radiation (Ruschy et al. 1991), as well as a lifting of ceiling heights and a decrease in the percentage of coverage of clouds (Karl et al. 1993). All of these changes enhance the amount of radiation absorbed at the surface during the day and thus favor a more rapid rise in daily maximum temperature than in daily minimum temperature. The abrupt leveling off of the DTR after the spring peak, which occurs despite a continued increase in net radiation and decrease in cloudiness (Ruschy et al. 1991), has been linked to the seasonal onset of the growing season. Schwartz and Karl (1990), Schwartz (1992), and Schwartz (1996) analyzed changes in the atmospheric boundary layer relative to observed first-leaf emergence dates for cloned species of lilac at stations across eastern North America. According to these studies, atmospheric water vapor increases following the first-leaf date, and the rise in the daily maximum surface air temperature slows relative to the rise in 850–700-mb thickness. The authors conclude that the increase in atmospheric humidity may reflect an enhancement of surface evapotranspiration rates as a result of the onset of foliage production, and that the increase in the surface latent heat flux, in turn, suppresses daytime temperatures and the DTR. Since transpiration rates tend to rise with increasing net incoming solar radiation, and moisture tends to be abundant in the eastern United States during summer, the importance of this effect may be expected to increase until midsummer and then decrease during late summer and autumn, particularly after the senescence of vegetation (Xue et al. 1996). However, Schwartz (1992) also notes that the meridional wind becomes southerly approximately one week before the first-leaf date. Dai et al.'s (1999) results show that during autumn, winter, and spring, the advection of air masses with widely differing humidity and DTR characteristics may mask some of the radiative effects on the DTR. Thus, the role of temperature and moisture advection in modifying the DTR is unclear.

In this article, we analyze daily surface and 850-mb data over the eastern United States in search for further evidence of the influence of transpiration from vegetation on seasonal variations in the DTR. Our strategy is to 1) examine the distance between the spring and fall peaks in DTR climatologies for various latitude bands in relation to the length of the growing season, 2) determine whether atmospheric changes around the time of the autumn DTR peak mirror those observed during spring, and 3) stratify the data according to the percent of possible sunshine in order to separate the influence of cloudiness on the DTR from other effects. The consideration of both spring and fall changes may permit the extension of Schwartz's findings to include the effects of vegetation on the DTR throughout the growing season.

2. Data

The data used in this study consist of daily surface observations of daily maximum temperature (°F), daily minimum temperature (°F), and percent of possible sunshine at selected First Order Summary of the Day stations across a large portion of the eastern United States (National Climatic Data Center 1999) as well as 0000 and 1200 UTC 850-mb temperatures (K) and geopotential heights (m) from the National Centers for Environmental Prediction–National Center for Atmospheric Research (NCEP–NCAR) reanalysis project (Kalnay et al. 1996). The twice-daily 850-mb temperatures and geopotential heights on a 2.5° lat × 2.5° long grid were extracted from global four-times daily pressure level

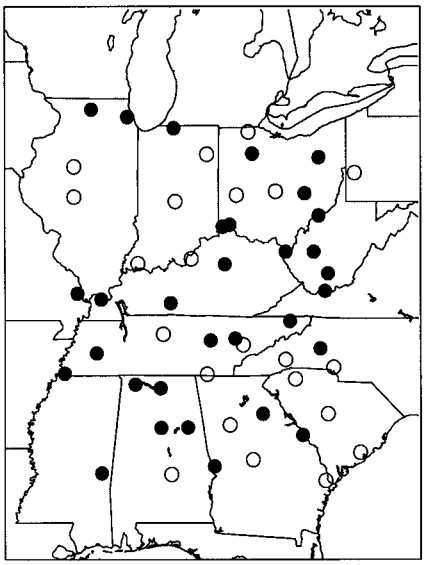

FIG. 1. Map of stations used in this study. Open circles indicate locations of stations with sunshine data. Closed circles mark all other stations.

data files archived at the NOAA–CIRES Climate Diagnostics Center. A detailed description of the reanalysis data and possible sources of error can be found online at http://wesley.wwb.noaa.gov/reanalysis.html as well as in Kalnay et al. (1996). For the purpose of this study, all surface and 850-mb temperatures have been converted to degrees Celsius.

Stations whose record of daily maximum and minimum temperatures between 1966 and 1995 is at least 90% complete and which lie within the area of the eastern United States in which the DTR climatology exhibits the characteristic warm season dip are included in this study. In addition, the area of study is adjusted to match the resolution of the NCEP data. The result is a set of 53 stations within the area 31.25°–43.75°N, 80°–90°W (Fig. 1). When analyses are restricted to mostly sunny days, only the 22 stations whose 1996–95 record of percent of possible sunshine is at least 90% complete are used. These stations are identified by open circles in Fig. 1.

In an attempt to emphasize variations that may be caused by fluctuations in surface processes, time series of ''relative surface air temperature'' have been computed for the late afternoon and early morning from daily maximum and minimum surface air temperatures at each station together with 0000 and 1200 UTC 850-mb temperatures and geopotential heights at the nearest NCEP reanalysis grid point. For each record, the 850-mb temperature (T_{850}) is projected onto the surface by adding to it the product of the dry-adiabatic lapse rate ($\Gamma_d = 9.8 \times 10^{-3}$ °C m^{-1}) and the 850-mb level's height (z_{850}) above the surface (z_s). The resulting reference temperature is then subtracted from the corresponding observed surface air temperature to obtain the relative surface temperature (T_r). Morning T_r [T_r(am)] is derived from daily minimum temperature ($T_{\min}$) and the same day's 1200 UTC 850-mb temperature and height, while afternoon T_r [T_r(pm)] is derived from daily maximum temperature ($T_{\max}$) and the corresponding 0000 UTC 850-mb data:

$$T_r(\text{am}) = T_{\min} - \{T_{850}(1200\ \text{UTC}) + \Gamma_d \times [z_{850}(1200\ \text{UTC}) - z_s]\},$$

$$T_r(\text{pm}) = T_{\max} - \{T_{850}(0000\ \text{UTC}) + \Gamma_d \times [z_{850}(0000\ \text{UTC}) - z_s]\}. \quad (1)$$

Positive (negative) values of T_r indicate that the lapse rate between the surface and the 850-mb level is steeper (less steep) than the dry-adiabatic lapse rate. An increase (decrease) in T_r therefore represents either a warming (cooling) of the surface relative to the atmospheric boundary layer or a cooling (warming) of the 850-mb level relative to the surface. As discussed in the previous section, enhanced surface evapotranspiration rates, for example, would act to decrease T_r(pm) by inhibiting daytime surface heating, while leaving T_r(am) unchanged. Any potential differential radiative effects of clouds at the surface and 850-mb level will be minimized by restricting the analysis of T_r to mostly clear days. Differences in temperature advection at the two levels, which may be significant in certain synoptic situations, are likely to average out in the climatological mean.

3. Results

Figure 2 shows the climatologies of the DTR between 80° and 90°W for five adjacent latitude bands centered at 42.5°, 40.0°, 37.5°, 35.0°, and 32.5°N. The climatological mean for each station is determined by computing, for each day of the year, the arithmetic mean of the differences between daily maximum and minimum temperatures. The resulting daily means are then averaged over the stations located within each of the five areas. Progressing from north to south, the character of the annual cycle of the DTR clearly changes: the distance between the two peaks widens during the warm half of the year, the summer dip becomes more pronounced, and the winter minimum becomes less prominent. In the northern two latitude bands, the spring maximum is larger than the autumn maximum, whereas the maxima are of comparable magnitude farther to the south. Based on the findings of the studies cited in section 1, the factors that may contribute to these seasonal and geographical variations in the DTR include net incoming solar radiation at the top of the atmosphere, cloudiness, and evapotranspiration from soil and vegetation.

All other things being equal, an increase in both daily net incoming solar radiation and the length of the day results in enhanced daytime surface heating, while a

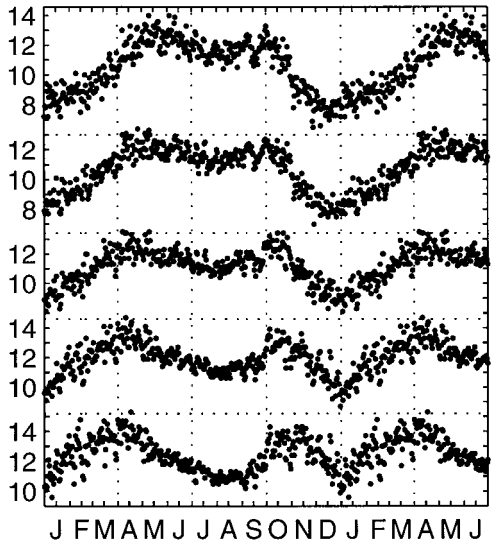

FIG. 2. Climatology of the diurnal temperature range (DTR, °C) for 2.5° lat bands between 80° and 90°W over the eastern United States. From top to bottom, the plots are for latitude bands centered at 42.5°, 40°, 37.5°, 35°, and 32.5°N. Each plot represents 1.5 annual cycles. Each dot represents the 1966–95 average of the DTR for one day of the year.

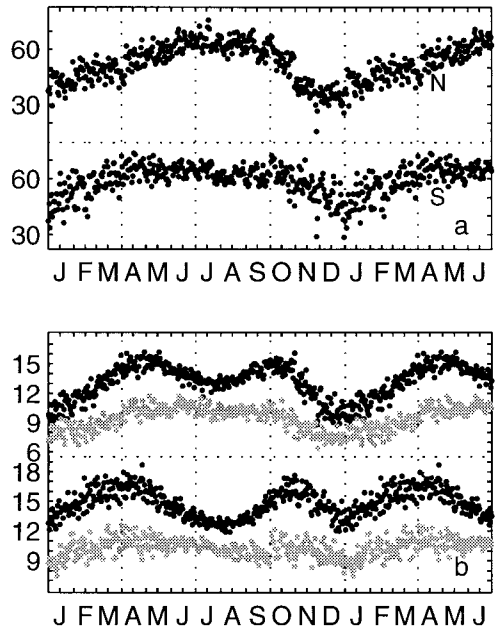

FIG. 3. (a) Climatologies of percent of possible sunshine (p_{sun}) for the 2.5° lat bands centered at 40° (N) and 35°N (S). (b) Climatologies of diurnal temperature range (°C) on mostly sunny ($p_{sun} > 75\%$; black) and other ($p_{sun} \leq 75\%$; gray) days for the same two latitude bands as in (a). Each plot represents 1.5 annual cycles. Each dot represents the 1966–95 average for one day of the year.

shortening of the night favors a reduction in radiative cooling and, therefore, a rise in daily minimum temperature. The former effect tends to outweigh the latter (e.g. Ruschy et al. 1991). Thus, based on seasonal changes in net incoming solar radiation and the number of daylight hours alone, one would expect the DTR to be at a minimum in winter and at a maximum in summer, and the amplitude of this seasonal cycle to decrease from north to south. Indeed, the wintertime DTR values tend to be larger in the south than in the north, whereas the summertime values do not increase toward the south. However, the largest values of the DTR are not observed around the time of the summer solstice.

The annual cycle of net shortwave and longwave radiation at the surface is modulated by changes in cloudiness. Figure 3a shows the climatology of the percent of possible sunshine (p_{sun}) for the 2.5°-wide latitude bands centered at 40° and 35°N, which are representative of the northern and southern portions of the study area. Each climatology constitutes an average over seven stations. Here p_{sun} is a measure of the duration of sunshine and is expressed as a percentage of the time between sunrise and sunset. Thus, variations in the percent of possible sunshine are closely related to variations in total cloud amount (Angell 1990; Karl and Steurer 1990; Plantico et al. 1990). While both plots in Fig. 3a exhibit a minimum during winter, the amplitude of the seasonal cycle and timing of the maximum in the two regions differ. The annual march is more pronounced in the north, mainly due to lower winter values. The plot of p_{sun} reaches its maximum during summer in the 40° lat band, but remains nearly flat between April and October in the 35° lat band. These results are in agreement with published seasonal mean climatologies of total cloud amount and sunshine duration over the eastern United States (Warren et al. 1986; Angell 1990).

Comparison of the shapes of the p_{sun} plots in Fig. 3a and the corresponding DTR climatologies, plotted as the second and fourth plots from the top in Fig. 2, shows a strong correspondence between seasonal variations of the two variables during the cold season. During the warm season, however, the shapes of the p_{sun} and DTR plots differ significantly, indicating that cloudiness cannot be the decisive factor in determining the DTR during that half of the year. To further facilitate the assessment of the effects of seasonal changes in cloudiness on the DTR, the DTR climatologies for mostly sunny days ($p_{sun} > 75\%$) and all other days ($p_{sun} \leq 75\%$) have been plotted for the 40° and 35° lat bands in Fig. 3b. The climatologies for mostly sunny days, denoted by black dots, are computed by averaging, for each day of the year, only the DTR values that occur on days with $p_{sun} > 75\%$.

Except on a few days during December and January in the 40° lat band, the average DTR is clearly higher on mostly sunny days than on other days. This difference reflects the efficiency with which clouds inhibit the daytime rise of surface air temperature by reducing the amount of shortwave radiation that reaches the surface. The relatively small effect of cloudiness on the DTR during midwinter in the north is likely to be in

part a result of relatively low incoming solar radiation (Dai et al. 1999). Since the amount of wintertime incoming solar radiation is larger in the southern region, cloudiness has a stronger influence on the DTR there. Overall, the characteristic seasonal maxima and minima in the DTR are more pronounced in the climatologies for mostly sunny days than in the other-day climatologies. If changes in cloudiness were responsible for the warm season dip in the DTR, then the amplitude of this dip should be reduced, if not eliminated, in the sunny-day DTR climatology. Instead, the dip is more prominent for $p_{sun} > 75\%$ (Fig. 3b, black) than for all days (Fig. 2) and is virtually absent when only days with $p_{sun} \leq 75\%$ are considered (Fig. 3b, gray). Furthermore, the dip remains prominent even when the DTR climatology is calculated using days on which p_{sun} exceeds 99%. Together, these results indicate that although cloudiness plays a significant role in determining the DTR on a day-to-day basis within a particular season (Plantico et al. 1990; Dai et al. 1999), it does not account for the peculiar character of the annual march of the DTR in the eastern United States. This conclusion is in agreement with Leathers et al.'s (1998) finding that cloud amount does not explain a significant portion of the variance in the DTR's annual cycle. The pronounced warm season dip in the sunny-day DTR climatologies further suggests that this dip is caused by a process that limits the ability of solar radiation to heat the surface during the day and whose effect is particularly strong during summer. Since, as discussed in section 1, the magnitude of the DTR is primarily determined by processes that control the heating of the surface by incoming solar radiation, seasonal changes in longwave radiative fluxes are not likely to be important here.

The north-to-south progression of the climatological peaks in the DTR toward earlier in the spring and later in the fall (Fig. 2) is consistent with a lengthening of the growing season from north to south. In order to obtain a more quantitative measure of the change in the warm season interpeak distance, the dates of occurrence of the spring and autumn maxima at each station were computed from DTR climatologies that have been smoothed with a 5-day running mean. These dates were then averaged over each of the five latitude bands, and the difference between the autumn and spring dates was determined. The results, shown in Table 1, confirm the impression gained from Fig. 2. As the spring peak moves from late May in the north to mid-April in the south, the autumn peak shifts from late September to early November, and the interpeak difference increases from 4 months (124 days) to nearly 7 months (203 days). Similar results were obtained when the same analysis was conducted for sunny-day DTR climatologies (not shown), again indicating that the timing of the peaks is independent of variations in cloudiness.

A map of 30-yr-average first-leaf emergence dates of three cloned species of lilac and honeysuckle over a portion of eastern North America (Eastern North America Phenology Network 1999) shows a north-to-south change similar to that of the DTR's spring maximum. The first-leaf date shifts from late April in northern New England to early March in Tennessee and North Carolina. Since lilac and honeysuckle tend to be among the first plants to leaf out, the bulk of the leaves of all plants will probably not emerge until somewhat later. Thus, the timing of the DTR's spring maximum (Table 1) appears to be tied to the onset of the growing season. This association is consistent with Schwartz's hypothesis that increased evapotranspiration at the time of green-up may suppress the DTR through daytime evaporative cooling at the surface and may thus contribute to the change in slope of the DTR climatology during spring.

TABLE 1. Average dates of spring and autumn maxima in climatological mean diurnal temperature range (DTR) over the eastern United States (31.25°–43.75°N, 80°–90°W). Averages are for stations within 2.5° lat bands centered on the latitude (lat, °N) listed on the left. Dates are determined by separately finding the date of the maximum climatological mean DTR during Jan–Jun and Jul–Dec. Dates are given in yeardays (day) and as month/day (MM/DD). The differences (Diff) between the spring and autumn dates are given in days.

	Spring		Autumn		Diff
Lat	Day	MM/DD	Day	MM/DD	(Days)
42.5	144	05/24	268	09/25	124
40.0	133	05/13	272	09/29	139
37.5	117	04/27	285	10/12	168
35.0	107	04/17	294	10/21	187
32.5	107	04/17	310	11/06	203

In Fig. 4, climatologies of average daily maximum and minimum temperature (T_{max} and T_{min}) as well as afternoon and morning relative surface temperature [T_r(pm) and T_r(am)] on mostly sunny days ($p_{sun} > 75\%$) are displayed together with the sunny-day climatologies of the DTR and the daily range of relative surface temperature. The elimination of days with $p_{sun} \leq 75\%$ again minimizes the potential effects of variations in cloudiness on the plotted variables. For this figure, values have been averaged over all 22 stations within the study area for which sufficient sunshine data are available. Solid vertical lines mark the dates of the DTR maxima in the annual march. The time rate of change of relative surface temperature with calendar date, as defined in the previous section, indicates whether the surface is growing warmer or cooler relative to the 850-mb temperature and thus emphasizes the changes in surface temperature that are due to variations in surface processes. Since, in the climatological mean, diurnal variations in 850-mb temperature are small, the annual cycles of DTR and the diurnal range in T_r are virtually identical (a, c).

On mostly sunny days in spring, T_{max} and T_r(pm) increase rapidly with calendar date leading up to the DTR maximum (Figs. 4b,d). The slope in T_r(pm) begins to decrease at or just before the spring DTR peak, and the curve flattens out a few weeks later, whereas T_{max} increases steadily throughout the spring. These results

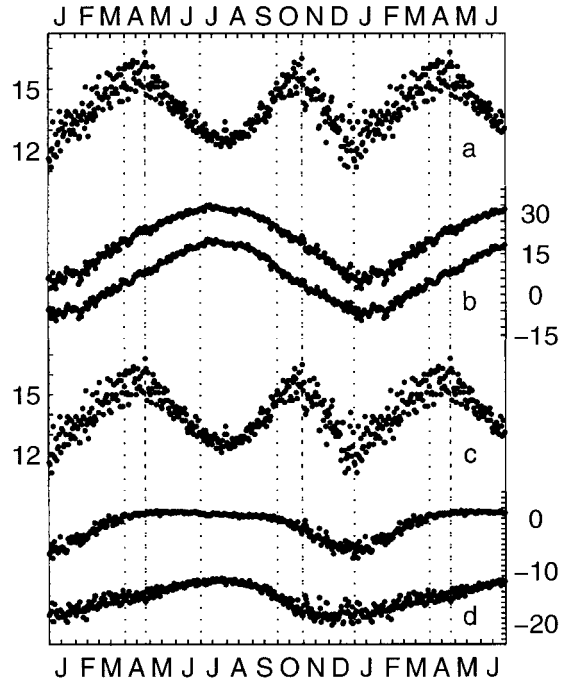

FIG. 4. Clear-day climatologies of (a) diurnal temperature range, (b) daily maximum and minimum surface air temperature, (c) the diurnal range of relative surface air temperature, and (d) afternoon and morning relative surface air temperature. Clear days are defined as days with percent of possible sunshine $> 75\%$. Each plot represents 1.5 annual cycles and an average over 22 stations within the study area. Solid vertical lines indicate dates of DTR maxima. All temperatures are in degrees Celsius. The period of record is 1966–95.

imply that after the DTR maximum, the seasonal warming of the surface relative to the warming of the lower atmosphere ceases during the day but continues at night. The daytime changes are similar to those found to take place following the emergence of leaves (Schwartz and Karl 1990; Schwartz 1996). Thus, it appears that the springtime reduction in the DTR is linked to the increase in evapotranspiration from emerging vegetation.

Climatologies of the weekly Normalized Difference Vegetation Index (NDVI; not shown) are in qualitative agreement with those of the DTR in the eastern United States during spring in that the DTR maximum usually occurs 1–2 weeks after the onset of a rapid increase in the NDVI. It is unclear why the DTR maximum does not occur shortly before or exactly at the time of green-up. One possible explanation is a discrepancy between satellite-based measurements of the spring green wave and surface phenology. Schwartz and Reed (1999) found that, over the eastern United States, satellite-based estimates of the start of the spring season consistently fell 1–2 weeks before first leaf emergence dates computed by his Spring Index Model. Perhaps the evapotranspiration from the first green leaves sensed by the satellite is not yet sufficient to suppress daytime temperatures in the presence of rapidly increasing clear-day solar radiation. However, a detailed comparison of the DTR and NDVI climatologies is not possible because the determination of the exact time of green-up from the NDVI is complicated by the various uncertainties in the NDVI data, the biweekly resolution of the NDVI, and a dependence of the NDVI on vegetation type, soil type, and illumination (Reed et al. 1994).

Throughout the summer, the abundant precipitation in this region combined with high temperatures continues to favor high evapotranspiration rates and relatively low values of T_r(pm) and DTR. Thus, evapotranspiration from soil and vegetation may be responsible not only for the change in slope of the DTR climatology in spring, but also for the subsequent warm season dip in the DTR. The changes in the slopes of $T_{\max}$, $T_{\min}$, T_r(pm), and T_r(am) around the time of the autumn DTR peak represent a reversal of the changes observed in spring. A temporary enhancement of daytime surface heating as a result of the gradual senescence of vegetation may, in part, explain the observed autumn change in afternoon T_r and DTR. However, in agreement with Schwartz's (1990) report of a weaker association during autumn between meteorological conditions and phenological events in honeysuckle and lilac, the signal in afternoon T_r is less pronounced in autumn than in spring. A likely reason for the weaker autumn relationship is that the photosynthetic activity of tall grasses, shrubs, and trees peaks in late spring or early summer and is affected by the amount of moisture available throughout the warm season (Reed et al. 1994), so that the decrease in greenness at the time of senescence is more gradual than the rate of increase during green-up. After the disappearance of green vegetation, the rapidly declining insolation causes the DTR to decline toward its winter minimum.

4. Concluding remarks

In conclusion, the warm season dip in the DTR appears to be a result of high evapotranspiration rates from vegetation during the day, which increase rapidly at the onset of the growing season in spring and continue to be high throughout much of the summer. Before the spring maximum and after the autumn maximum in the DTR, seasonal DTR variations appear to be controlled largely by seasonal changes in insolation and cloudiness. These findings support Mearns et al.'s (1995) suggestion that the correct simulation of seasonal variations in the DTR, especially during the warm half of the year, requires a detailed and realistic parameterization of soil–vegetation–atmosphere interactions.

Further improvements in the quality of the NDVI and an expansion of ground-based observations of land surface conditions would greatly aid the ability to determine climatological relationships between changes in vegetation and atmospheric conditions. New and expanded surface phenological observing networks that also report measurements of surface evapotranspiration

and meteorological variables would be particularly useful in such research efforts.

Acknowledgments. We thank the reviewers for their helpful comments and suggestions. The work was supported by the National Science Foundation through the Climate Dynamics Program under Grant ATM-9805886. NCEP–NCAR reanalysis data were provided by the NOAA–CIRES Climate Diagnostics Center, Boulder, Colorado (http://www.cdc.noaa.gov/).

REFERENCES

Angell, J. K., 1990: Variation in United States cloudiness and sunshine duration between 1950 and the drought year of 1988. *J. Climate,* **3,** 296–308.

Campbell, G. G., and T. H. Vonder Haar, 1997: Comparison of surface temperature minimum and maximum and satellite measured cloudiness and radiation. *J. Geophys. Res.,* **102,** 16 639–16 645.

Cao, H. X., J. F. B. Mitchell, and J. R. Lavery, 1992: Simulated diurnal range and variability of surface temperature in a global climate model for present and doubled CO_2 climates. *J. Climate,* **5,** 920–943.

Dai, A., K. E. Trenberth, and T. R. Karl, 1999: Effects of clouds, soil moisture, precipitation and water vapor on diurnal temperature range. *J. Climate,* **12,** 2451–2473.

Dorman, J. L., and P. J. Sellers, 1989: A global climatology of albedo, roughness length, and stomatal resistance for atmospheric general circulation models as represented by the Simple Biosphere Model (SiB). *J. Appl. Meteor.,* **28,** 833–855.

Eastern North America Phenology Network, cited 1999: 30-year normal first-leaf date map (three-plant average). [Available online at http://www.uwm.edu/~mds/enanet.html.]

Gaffen, D. J., and R. J. Ross, 1999: Climatology and trends of U.S. surface humidity and temperature. *J. Climate,* **12,** 811–828.

Kalnay, E., and Coauthors, 1996: The NCEP/NCAR 40-Year Reanalysis Project. *Bull. Amer. Meteor. Soc.,* **77,** 437–471.

Karl, T. R., and P. M. Steurer, 1990: Increased cloudiness in the United States during the first half of the twentieth century: Fact or fiction? *Geophys. Res. Lett.,* **17,** 1925–1928.

——, and Coauthors, 1993: A new perspective on recent global warming: Asymmetric trends of maximum and minimum temperature. *Bull. Amer. Meteor. Soc.,* **74,** 1007–1023.

Kaufmann, M. R., 1984: A canopy model (RM-CwW) for determining transpiration of subalpine forests. Part II: Consumptive water use in two watersheds. *Can. J. For. Res.,* **14,** 227–232.

Kukla, G., J. Gavin, M. Schlesinger, and T. Karl, 1995: Comparison of observed seasonal temperature maxima, minima, and diurnal range in North America with simulations from three global climate models. *Atmos. Res.,* **37,** 267–275.

Leathers, D. J., M. A. Palecki, D. A. Robinson, and K. F. Dewey, 1998: Climatology of the diurnal temperature range annual cycle in the United States. *Climate Res.,* **9,** 197–211.

Mearns, L. O., F. Giorgi, L. McDaniel, and C. Shields, 1995: Analysis of variability and diurnal range of daily temperature in a nested regional climate model: Comparison with observations and doubled CO_2 results. *Climate Dyn.,* **11,** 193–209.

National Climatic Data Center (NCDC), cited 1999: Summary of the day—First Order: TD-3210 online data format documentation. [Available online at ftp.ncdc.noaa.gov.]

Oliver, S. A., H. R. Oliver, J. S. Wallace, and A. M. Roberts, 1987: Soil heat flux and temperature variation with vegetation, soil type and climate. *Agric. For. Meteor.,* **39,** 257–269.

Plantico, M. S., T. R. Karl, G. Kukla, and J. Gavin, 1990: Is recent climate change across the United States related to rising levels of anthropogenic greenhouse gases? *J. Geophys. Res.,* **95,** 16 617–16 637.

Radersma, S., and N. de Reider, 1996: Computed evapotranspiration of annual and perennial crops at different temporal and spatial scales using published parameter values. *Agric. Water Man.,* **31,** 17–34.

Reed, B. C., J. F. Brown, D. Vanderzee, T. R. Loveland, J. W. Merchant, and D. O. Ohlen, 1994: Measuring phenological variability from satellite imagery. *J. Veg. Sci.,* **5,** 703–714.

Robinson, D. A., D. J. Leathers, M. A. Palecki, and K. F. Dewey, 1995: Some observations on climate variability as seen in daily temperature structure. *Atmos. Res.,* **37,** 19–31.

Ruschy, D. L., D. G. Baker, and R. J. Skaggs, 1991: Seasonal variation in daily temperature ranges. *J. Climate,* **4,** 1211–1216.

Saltzman, B., and J. A. Pollack, 1977: Sensitivity of the diurnal surface temperature range to changes in physical parameters. *J. Appl. Meteor.,* **16,** 614–619.

Schwartz, M. D., 1990: Detecting the onset of spring: A possible application of phenological models. *Climate Res.,* **1,** 23–29.

——, 1992: Phenology and springtime surface-layer change. *Mon. Wea. Rev.,* **120,** 2570–2578.

——, 1996: Examining the spring discontinuity in daily temperature ranges. *J. Climate,* **9,** 803–808.

——, and T. R. Karl, 1990: Spring phenology: Nature's experiment to detect the effect of ''green-up'' on surface maximum temperatures. *Mon. Wea. Rev.,* **118,** 883–890.

——, and B. C. Reed, 1999: Surface phenology and satellite sensor-derived onset of greenness: An initial comparison. *Int. J. Remote Sens.,* **20,** 3451–3457.

Stenchikov, G. L., and A. Robock, 1995: Diurnal asymmetry of climatic response to increased CO_2 and aerosols: Forcings and feedbacks. *J. Geophys. Res.,* **100,** 26 211–26 227.

Verdecchia, M., G. Visconti, F. Giorgi, and M. R. Marinucci, 1994: Diurnal temperature range for a doubled carbon dioxide concentration experiment: Analysis of possible physical mechanisms. *Geophys. Res. Lett.,* **21,** 1527–1530.

Warren, S., C. Hahn, J. London, R. Chervin, and R. Jenne, 1986: Global distribution of total cloud cover and cloud type amounts over land. NCAR Tech. Note NCAR/TN-273 + STR and DOE Tech. Rep. DOE/ER/60085-H1, U.S. Department of Energy, Carbon Dioxide Research Division, Washington, DC, 29 pp. [Available as numeric data package NDP-026 from Carbon Dioxide Information Analysis Center, Oak Ridge National Laboratory, P.O. Box 2008, Oak Ridge, TN 37831-6050.]

Xue, Y., M. J. Fennessy, and P. J. Sellers, 1996: The impact of vegetation properties on U.S. summer weather prediction. *J. Geophys. Res.,* **101,** 7419–7430.